Entergy

**Entergy Nuclear South**
Entergy Operations, Inc.
17265 River Road
Killona, LA 70057-3093
Tel 504-739-6660
Fax 504-739-6678
jkowale@entergy.com

**Joseph A. Kowalewski**
Vice President, Operations
Waterford 3

W3F1-2010-0064

August 12, 2010

U.S. Nuclear Regulatory Commission
Attn: Document Control Desk
Washington, DC 20555

SUBJECT: Response to NRC Requests for Additional Information Regarding License Amendment Request for Leak-Before-Break of the Pressurizer Surge Line
Waterford Steam Electric Station, Unit 3
Docket No. 50-382
License No. NPF-38

REFERENCES:
1. W3F1-2010-0003, Entergy letter dated February 22, 2010, "License Amendment Request for Approval of Leak-Before-Break of the Pressurizer Surge Line" (ADAMS Accession No. ML100550606).
2. Electronic Communication dated April 21, 2010, NRC Request for Additional Information on Waterford 3 Licensee Amendment Request for Approval of Leak-Before-Break of the Pressurizer Surge Line (ADAMS Accession No. ML101110635).

Dear Sir or Madam:

By letter dated February 22, 2010 (Reference 1), Entergy Operations, Inc. (Entergy) requested NRC review and approval of a proposed license amendment to eliminate the dynamic protection requirements for the Waterford Steam Electric Station, Unit 3 (Waterford 3) pressurizer surge line. This request was prepared in accordance with General Design Criterion (GDC) 4, "Environmental and Dynamic Effects Design Bases" using the guidance of Standard Review Plan (SRP) 3.6.3, "Leak-Before-Break Evaluation Procedures" (NUREG-0800). The Waterford 3 pressurizer Leak-Before-Break (LBB) surge line analyses were provided in Westinghouse WCAP-17187-P, "Technical Justification for Eliminating Pressurizer Surge Line Rupture as the Structural Design Basis for Waterford Steam Electric Station, Unit 3, Using Leak-Before-Break Methodology."

On April 21, 2010 (Reference 2), the NRC staff issued a Request for Additional Information to Entergy in order to complete review of the license amendment request. Entergy electronically provided responses to the NRC requests on June 8, 2010. Based on further NRC review of Entergy's responses, the NRC issued a subsequent Request for Additional Information that was electronically provided to Entergy on June 23, 2010. A conference call was conducted between members of the NRC Staff, Entergy, and Westinghouse Electric Company on July 16, 2010 to discuss proposed resolutions to the subsequent requests. These proposed

A001
NRR

resolutions were based on talking notes provided to the NRC prior to the call by Entergy. As agreed on the July 16, 2010 call, Entergy would formally document previous communications on the Waterford 3 docket. Therefore, Entergy is hereby providing the NRC Requests for Additional Information and our responses as contained in Attachment 1 of this letter.

The letter contains no new commitments and no information that is Proprietary. If you have any questions or require additional information, please contact William J. Steelman at 504-739-6685.

I declare under penalty of perjury that the foregoing is true and correct. Executed on August 12, 2010.

Sincerely,

JAK/SAB

Attachments:
1. Response to NRC Requests for Additional Information for License Amendment Request Regarding Leak-Before-Break of the Waterford 3 Pressurizer Surge Line

cc: Mr. Elmo E. Collins, Jr.
Regional Administrator
U. S. Nuclear Regulatory Commission
Region IV
612 E. Lamar Blvd., Suite 400
Arlington, TX 76011-8064

NRC Senior Resident Inspector
Waterford Steam Electric Station, Unit 3
P.O. Box 822
Killona, LA 70066-0751

U.S. Nuclear Regulatory Commission
Attn: Mr. N. Kalyanam
MS O-07 D1
Washington, DC 20555-0001

**Attachment 1 to**

**W3F1-2010-0064**

**Response to NRC Requests for Additional Information for License Amendment Request Regarding Leak-Before-Break of the Waterford 3 Pressurizer Surge Line**

**Response to NRC Requests for Additional Information for License Amendment Request Regarding Leak-Before-Break of the Waterford 3 Pressurizer Surge Line**

The NRC Staff issued Requests for Additional Information (RAIs) of April 21, 2010 and June 23, 2010, regarding Entergy's February 22, 2010 application to amend the Waterford 3 operating license for the elimination of dynamic affects of the Waterford 3 surge line based on the requirements of General Design Criteria 4. This attachment documents these NRC RAIs and the Entergy responses to these requests. Note that the subsequent June 23, 2010 Request for Additional Information and Entergy responses are provided after the initially numbered RAIs and are denoted as Round 2.

**RAI N-1** Discuss whether the reactor coolant system (RCS) leakage detection system capability of 0.25 gallons per minute (gpm) is applicable for 1 hour or for 4 hour. Discuss the requirements of the Waterford technical specifications on the RCS leakage detection systems.

**Response:** The containment sump level Plant Monitoring Computer (PMC) computer point being credited for surge line leak-before-break (LBB) leakage detection is the same computer point that is used for the containment sump level leak detection capability for Technical Specification (TS) 3/4.4.5, "RCS Leakage Detection Instrumentation." The sump level computer point was approved by the NRC in Waterford 3 Operating License Amendment 197 dated July 30, 2004 (ADAMS Accession No. ML042150057). This PMC containment sump computer point for TS 3/4.4.5 compliance is based on the ability to detect a one gpm containment inflow rate within one hour consistent with response time requirements in Regulatory Guide (RG) 1.45 which satisfies General Design Criterion (GDC) 30. The installed containment sump instrumentation is sensitive enough to detect less than a 0.25 gpm change in leakage rate within 20 minutes (< one gpm within one hour). This is based on conservatively combining reference accuracies of individual instrument loop components and averaging the combination over 300 scans, (one scan per second over five minutes). This is compared to the next five minute scan average. Accounting for a 10 minute containment sump draw-down, conservative minimum time to detect a change is 20 minutes. This sensitivity is acceptable for detecting increases in unidentified leakage for surge line LBB. However, the 0.25 gpm leakage detection sensitivity for LBB acceptability is not directly related to the TS required monitoring function as discussed below.

Section III.4 of Standard Review Plan 3.6.3 (Revision 1) for LBB states:

> Leakage detection systems are evaluated to determine whether they are sufficiently reliable, redundant, and sensitive so that a margin on the detection of unidentified leakage exists for through-wall flaws to support the deterministic fracture mechanics evaluation. The specifications for plant-specific leakage detection systems inside the containment should be equivalent to those in RG 1.45, "Reactor Coolant Pressure Boundary Leakage Detection Systems."

The NRC guidance contained in Revision 1 of RG 1.45 distinguishes between that which is required for normal RCS unidentified leakage under GDC 30 and that required for a specific LBB application for compliance to GDC 4. For LBB applications, Revision 1 of RG 1.45 does not specify either a one hour or 4 hour response criteria. The LBB response time for a specific piping application are based on meeting the results of the LBB analyses (RG 1.45, Revision 1, page 8) which states:

If leak-before-break (LBB) analysis is approved for the plant, the overall response time of the leakage monitoring system should be sufficient to support the LBB analysis procedures.

This approach is appropriate since the analyses are based on known piping and weld material properties and stress profiles for the specific analyzed piping segment. As discussed in WCAP-17187-P, the Waterford 3 surge line remains stable with acceptable margin. Therefore, detection sensitivity is the primary factor for meeting the surge line analytical results. Given the sensitivity of the containment sump level computer point to monitor as low as 0.1 gpm (< 0.25 gpm) and the Waterford 3 RCS unidentified leakage monitoring program including action levels routinely performed per the guidance of WCAP-16465, Waterford 3 complies with GDC 4 and RG 1.45 (Revision 1) guidance.

**RAI N-2** Page 2-3, Section 2.4 discusses thermal stratification of the surge line. Thermal stratification is a form of thermal-induced fatigue. SRP Section 3.6.3.III.10 does not permit LBB applied to piping with a history of fatigue cracking or failure. Explain why LBB is applicable to the pressurizer surge line considering thermal fatigue exists in the pipe.

**Response:** Based on known data there has been no cracking in either Westinghouse or Combustion Engineering (CE)-Fleet surge lines. There was one case in 1989 where the Trojan plant replaced a surge line nozzle for what was believed to have been a flaw. Subsequent examination of the nozzle did not identify any flaws. Therefore, there is no known history of surge line cracking. Additionally, a review of inservice inspections for the attached components located on the Waterford 3 surge line has not revealed any reportable indications (flaws).

The issue of thermal stratification in the surge line was initially documented in NRC Bulletin 88-11. Entergy responded to the NRC in letter dated March 3, 1989 (W3P89-0057) indicating that Waterford 3 would participate in addressing several action items agreed on by the Combustion Engineering Owners Group (CEOG) and the NRC Staff. In essence, Entergy participated in supplying plant data to support a bounding analysis of CEOG surge lines, which met the reporting requirements in the bulletin.

Subsequently, Entergy provided the results of a visual inspection of the surge line, which concluded that neither the surge line nor its affiliated hardware had suffered any discernable distress or structural distress as a result of thermal stratification (W3F1-92-0135 dated May 5, 1992). In addition, it was noted that the generic bounding analysis performed by the CEOG (CEN-387-P, Revision 1) bounded the Waterford 3 surge line. Therefore, the only remaining Bulletin action item pertaining to Waterford 3 was to perform plant specific activities to update surge line design documentation.

This action was completed and reported to the NRC (W3F1-93-0371 dated 12/23/1993), demonstrating that the integrity of the Waterford 3 pressurizer surge line satisfied ASME Section III criteria for the life of the plant, taking into account the effects of thermal stratification. As a result of the ASME Code analyses and the absence of any indications of fatigue cracking in the Waterford 3 surge line, the existence of thermal fatigue does not preclude the application of LBB.

**RAI N-3** Page 3-3, Section 3.4, first paragraph, states that the applied loads for the surge line LBB analysis are obtained from Waterford updated pipe stress reanalysis.

(a) Discuss the updated stress reanalysis, including whether the pipe loadings as a result of the proposed steam generator replacement and NRC-approved power uprate are included in the updated analysis.

(b) Discuss the impact of the steam generator replacement and power uprate conditions on the pipe supports, routing, and their locations on the surge line.

**Response:** (a) The stress and fatigue analyses for the Waterford 3 (W3) surge line were updated for the effects of extended power uprate (EPU), and for the effects of EPU and replacement steam generators (RSGs). In both cases they were found to be acceptable.

The original analysis performed for EPU considered normal operation (NOp) deadweight and thermal loads which were reconciled for the effects of EPU. The design basis loads and thermal anchor motions (TAMs) were changed where necessary. EPU did not have a significant effect on the seismic response of the system, so the seismic design basis RCS loads and seismic anchor motions (SAMs) were retained. New branch line pipe break (BLPB) input forcing functions were developed and analyzed for their effects on the RCS (i.e., to determine new RCS loads and BLPB anchor movements (BAMs)).

These RCS responses (hot leg surge nozzle seismic and BLPB excitations, and surge line TAMs, SAMs and BAMs) were used as inputs to the surge line reanalysis, along with the appropriate thermal stratification transient inputs (see response to RAI Item N-5 a) to update the design basis for EPU conditions. Surge line stresses were found to be acceptable for EPU conditions.

The Waterford 3 RCS design basis was reanalyzed for the replacement SGs. Separate RCS analyses were performed for the effect of RSGs on seismic, BLPB, and NOp system response. The surge line was then reanalyzed for the updated seismic, BLPB, and NOp inputs and the effects of thermal stratification and were found to be acceptable.

(b) No changes in the surge line routing, pipe supports (i.e., dead weight hangers), and pipe whip restraints were required for either EPU, or EPU with RSG conditions.

The current analysis of the Waterford 3 surge line for the application of LBB is based on the latest set of design basis loads, which are for EPU with RSG conditions. There were some changes in the load and stress results with inclusion of RSGs. However, all ASME Code requirements continue to be met, and the resulting fatigue usage, 0.41, is well below the Code allowable of 1.0.

**RAI N-4** Page 3-3, Section 3.4 states that load cases A, B, and C are normal operation conditions and D, E, F, and G are faulted conditions. There should be 12 loading combinations of normal operation conditions plus faulted conditions: A/D, A/E, A/F, A/G, B/D, B/E, B/F, B/G, C/D, C/E, C/F, and C/G. The report states that load cases C and G are for information only. This leaves the loading combinations of A/D, A/E, A/F, B/D, B/E, and B/F. Explain why load combinations A/E and B/D were not shown in Table 3-4.

**Response:** For the Waterford 3 pressurizer surge line LBB application with stratification loadings, Westinghouse established the various loading cases and combinations which have been accepted by the NRC in previous LBB applications. Section 3.4 and Tables 3-3 and 3-4 provide the loading scenario and possible combination cases. Loading Case E (faulted) has the normal operating steady state stratification loads that should be combined with loading Case B which has normal operating steady state stratification loads. Similarly, Loading Case D (faulted) has the normal operating thermal loads that should be combined with the normal operating loading Case A which has normal operating thermal loads. Therefore, the logical combinations are Case A/D and Case B/E and these combinations are appropriate for the LBB analyses and are considered acceptable.

**RAI N-5.** Page 3-4, second paragraph, discusses temperatures used for thermal stratification. However, it is not clear how the temperatures were derived. The maximum stratification temperature differential considered was X1 degrees F (temperatures in this paragraph are proprietary information). The bottom-to-top temperature on the pipe cross section was increased from X2 degrees F to X3 degrees F. A temperature of X5 degrees F for node 70 was estimated for the stratification high case. In the normal stratification case, the temperature increased from X4 degrees F to X3 degrees F.

(a) Explain how all these temperatures were derived.

(b) Provide the normal operation temperature at Node 10 (hot leg to surge line nozzle) and at Node 80 (pressurizer to surge line nozzle). Discuss whether thermal stratification occurs at Nodes 10 and 80.

(c) The footnote for Tables 3-3 and 3-5 states that the maximum stratification temperature differential of X1 degrees F was applied for information only. Discuss whether the maximum stratification temperature differential was included in calculating critical crack sizes in Tables 6-1 and 6-2 and leakage crack sizes in Tables 5-1 and 5-2. If the maximum stratification differential temperature was not included in deriving the critical and leakage crack size for the surge line, provide justification.

**Response:** (a) A CE Owners Group program gathered plant data and developed the methodology to determine the resulting temperatures in the surge line. This report (CE NPSD-546-P, Volume 1, "Pressurizer Surge Line Flow Stratification Evaluation," CEOG Task 587, July, 1989) evaluated the instrumentation data, and provided the basis and details of the resulting thermal hydraulic evaluation that is discussed in Section 3.3.4 of the report and is summarized below.

The derivation of the top-to-bottom fluid temperatures in the horizontal portions of the surge line was based on measured plant data from various CE-fleet plants. The most extensive measurements were taken at Calvert Cliffs Units 1 and 2, Fort Calhoun Station, and SONGS Units 2 and 3. Surface-mounted thermocouples (in many locations mounted circumferentially around the pipe at 60° intervals) were placed along the surge lines. Data was taken for both heatup and cooldown conditions. After data reduction was performed, temperature versus time plots were developed.

Since only the outside pipe wall temperature measurable data was collected, the inside fluid conditions were not explicitly known, and therefore needed to be calculated. Various fluid models were evaluated to determine what fluid conditions inside of the surge line produced the measured pipe wall temperature profiles. These evaluations produced the top-to-bottom fluid temperature differences characterized in the design basis thermal stratification transients. The transients were used in the stress and fatigue structural analyses of the piping, nozzles, and supports.

It was determined that a set of transients and associated cycles consisting of (X3-X4) °F steady state thermal stratification, normal stratification, and X1°F high and low stratification (i.e., maximum stratification occurring at the high and low ends of the ambient to X3°F temperature range in the surge line) was an adequate representation of the conditions observed during CE plant heatups and cooldowns.

These top-to-bottom temperature differences were applied along the entire length of the surge line horizontal run, along with a linear thermal expansion temperature input equal to the average of the top-to-bottom temperature difference. For example, a temperature of (X3 + X2)/2 was used as input for the thermal stratification high case. Since stratification in the vertical piping is negligible, loads in these portions of the surge line were only subjected to effects from linear thermal expansion. Again using the thermal stratification high case as an example, X3°F was applied to the pressurizer end of the model, and X2°F was applied to the hot leg end of the model.

(b) Nodes 10 and 80 represent the surge line/hot leg surge nozzle interface and the surge line/pressurizer surge nozzle interface, respectively. Node 10 was assumed to have a steady state normal operation temperature of X4°F and Node 80 has a steady state temperature of X3°F. These temperatures apply to the fluid when stratification is not occurring.

The surge line is oriented vertically at the reactor coolant system and pressurizer interfaces. Stratified flow cannot be maintained in the vertical sections of the piping; hence stratification is not assumed at Nodes 10 and 80.

(c) Loading Case F (faulted) has the maximum stratification temperature differential condition and this case was used for the critical flaw size determination. Case C (normal) has the maximum stratification temperature differential condition and the stress for Case C is significantly higher than the normal loading Case A and Case B. Loading Case C will provide significantly lower leakage flaw size. Lower leakage flaw size will provide higher LBB flaw size margin and therefore, Case C does not govern and Case A or Case B with lower normal stresses (which will provide higher leakage flaw sizes and eventually lower flaw size margins) govern.

**RAI N-6** Page 5-2, first paragraph, states that the crack relative roughness was obtained from fatigue crack data on stainless steel samples. Discuss the source of the stainless steel samples. Discuss how the roughness value was obtained.

**Response:** Westinghouse developed crack relative roughness values which have been previously accepted by the NRC. WCAP-9558 (Proprietary), Revision 2,

"Mechanistic Fracture Evaluation of Reactor Coolant Pipe Containing a Postulated Circumferential Through-wall Crack" dated May 1981 documented the crack relative roughness that was used for the fracture mechanics LBB leak rate calculations. Since 1981 Westinghouse has applied this crack relative roughness value for similar LBB applications.

**RAI N-7** Page 5-2, Section 5.4, first paragraph, states that the crack opening area was estimated using the method of Reference 5-3. Discuss in detail exactly how the crack opening area was estimated and provide page numbers in Reference 5-3 which show the crack opening area calculation.

**Response:** The crack opening areas were calculated based on NUREG/CR-3464, page 71-81. The crack opening area estimation is based on linear elastic fracture mechanics (LEFM), including effects of shell corrections. The imposed loads on the circumferential flaw are the axial tensile force and bending moment due to normal operating conditions (e.g. deadweight, pressure, thermal expansion). The crack opening area for the tensile loading is obtained by the energy method (Castigliano's theorem). The crack opening area for the bending load is obtained by further derivation as shown on pages 76 through 80 of NUREG/CR-3464. The two crack opening area components (tension and bending) are combined to determine the total crack opening area. Similarly, since 1981, Westinghouse has used this crack area calculation method for other LBB applications that have been reviewed by the NRC.

**RAI N-8** Page 5-3, first paragraph, states that the air-fatigue crack surge roughness of Y micro-inches (proprietary information) used for leak rate calculation by Westinghouse is about 50 percent higher than the typical surface roughness used by the industry. Discuss how the 50 percent is derived and discuss whether 50 percent is conservative.

**Response:** The air-fatigue crack surface roughness used for the leak rate calculation by Westinghouse [See Section 5.3 of WCAP-17187-P] is higher than the typical surface roughness of 200 micro-inches used by the industry in PICEP. WCAP-9558 substantiated the approach and basis for the higher surface roughness. Therefore, Westinghouse concludes that this air-fatigue crack surface roughness value is sufficiently conservative.

**RAI N-9** Page 5-3, (1) Explain why no penalty factor (P = 1.0) was applied to the Alloy 52M material in Equation 5-3. (2) Explain how penalty factor of 1.69 was derived from Reference 5-6 in the report because the staff derived a slightly higher penalty factor of 1.74 based on data in Reference 5-6.

**Response:** (1) The Alloy 52M weld overlay material is not susceptible to Primary Water Stress Corrosion Cracking (PWSCC) and a penalty factor of 1.0 (P=1) is appropriate for PWSCC.

(2) The penalty factor of 1.69 is taken directly from Slide 21 of Reference 5-6. Even though not stated, a linear least squares fit (y = ax type) was used to obtain the factor of 1.69.

The appropriateness and use of these factors are also addressed in the response to RAI N-10 below.

**RAI N-10** Page 5-3, The licensee derived the leakage crack size for the overlaid dissimilar metal weld of the surge line by multiplying an effective penalty factor (1.44) to the leakage crack size derived for the original dissimilar metal weld based on the fatigue degradation mechanism. The licensee derived the penalty factor (1.69) from the ratio of the leakage crack size derived for PWSCC and for fatigue in Reference 5-6. The staff questions the validity of this approach because in References 5-5 and 5-6, the leakage crack size was calculated for PWSCC and for fatigue without modeling an overlaid DMW. It appears that the licensee's approach was not verified by or based on any finite element or theoretical analysis. The licensee's approach may provide a rough estimate of the leakage crack size for the overlaid DMW. However, the staff expects that a fracture mechanics analysis would be performed to obtain the leakage crack size for the overlaid DMW, or at a minimum, the penalty-factor approach should be verified by a theoretical analysis. Justify application of the penalty factors.

**Response:** The approach taken by WCAP-17187-P applies previous industry recognized modeling techniques contained in Reference 5-5 (PVP2006-ICPVT11-93767, Nana and Yoon) and Reference 5-6 (Rudland, Wilkowski, et. al) to substantiate the application of conservative penalty factors. The WCAP uses these recognized industry initiatives to best estimate the effects of crack morphology for PWSCC susceptible Alloy 82/182 materials. Both of the referenced documents provide state of the art results given the data available and the focus of the study.

Reference 5-6 evaluates flow paths and flaw morphology of PWSCC flaw characteristics against previously applied LBB analyses to provide bounding leakage flaw penalty factors. The particular crack morphology parameters of interest are flaw roughness, number of turns, and actual flow path. Historically, leakage cracks were generally assumed to be characterized as fatigue cracks with the depth equal to the wall thickness. Reference 5-6 (See also PVP2005-71200 paper by the same authors) shows that circumferential Alloy 82/182 cracks are parallel to the long direction of dendritic grains which is considered a primary factor in PWSCC leakage flaw determination. Various crack growth photomicrographs are provided with emphasis on PWSCC and the individual crack types being characterized. The surface roughness, number of turns and actual flow path parameters are given in Slide 16 (Reference 5-6). Slide 17 provides the mean and standard deviation of the data obtained. However, these statistics produce a fairly wide variability in results from the data analyzed including that for PWSCC which can contribute to overly conservative results [local roughness ($\mu_L$, μm) with mean of 16.86 and std dev of 13.57, global roughness ($\mu_G$, μm) with mean of 113.9 and std dev =90.97, and number of turns ($n_L$, $mm^{-1}$) with mean of 5.94 and std dev of 4.54].

Only crack length parameters are closely banded. These numbers are the ratio of crack lengths to thicknesses and are stand-alone values. Reference 5-6 listed both $K_G$ (large crack opening displacement (COD) relative to global roughness) and $K_{G+L}$ (small COD relative to global roughness). The authors note only that the local and global roughnesses for the PWSCC cracks (growing parallel to the long direction of the dendritic grains) are higher than those for IGSCC cracks, while also noting that the number of turns is lower. This suggests that crack length factor (i.e., $K_{G+L}$) may

have a dominating role in the weld metal response to the PWSCC crack growth. The length of the actual flow path is simply $K_{G+L}$ times t (weld thickness).

The mean value for the leakage flow path for PWSCC cracks is 1.243, that is, the flow path is 24.3% greater than the thickness. It is further noted that for the PWSCC weld metal results, the standard deviation to mean ratio is 0.079/1.243=0.064. It is believed that as more data would be applied, the standard deviation would decrease with the mean remaining relatively constant.

The analyses and methodology of Reference 5-6 (and PVP2005-71200) provide an excellent approach to understanding the affects of leakage flaw sizing due to PWSCC. However, based on the limited data available the analyses are believed to provide overly conservative results. Specifically, the 69% increase in leakage flaw size is believed to be exaggerated due to lack of data as discussed below. Therefore, the use of a penalty factor of 1.69 for Alloy 82/182 materials in WCAP-17187-P is concluded to be conservative. Additionally, the use of a 1.69 penalty factor in Alloy 82/182 material is also recognized as being "very conservative" in Materials Reliability Program (MRP) Report 140, "Leak-Before-Break Evaluation for PWR Alloy 82/182 Welds (MRP-140)".

The objective of the study in Reference 5-5 was to determine the effect of percent increase in crack length when considering cracks with PWSCC morphology instead of the fatigue morphology assumed in most LBB analyses. This study is believed to provide a better representation of the affects of PWSCC in Alloy 82/182 materials. This is first based on the fact that the authors provide benchmarking results for their leak rate program KRAKFLO. Next, the laboratory test results for IGSCC leak rate studies were analyzed and were found to be in very good agreement with the measured and predicted leak rates with conservative predictions found for small leak rates. The further benchmarking performed for field data would tend to provide additional validation of the inputs. Finally, the authors performed a sensitivity study for five different piping systems containing Alloy 82/182 welds.

From an LBB perspective, KRAKFLO predicts on average, a 37% increase (ranged from 28% to 47%) in crack length when considering the crack with SCC morphology over conventional fatigue morphology. The standard deviation was 6.41% which suggests less scatter with the ratio of standard deviation to mean being 17.3%. The results of this approach provide a more highly validated penalty factor of 1.37 in fatigue leakage flaw size for LBB applications. It should be noted that IGSCC crack morphology which was used in this study is conservative since the PWSCC crack morphology is less severe than the IGSCC which is noted in Reference 5-6.

Based on the variability of results in Reference 5-6, the application of a penalty factor of 1.69 provides highly conservative results for the original weld joint. However, WCAP-17187-P applies this penalty factor conservatively in equation 5-3 for the thickness of the Alloy 82/182 material.

The design of the full structural weld overlays (SWOL) on the surge line piping is qualified for flaws extending through the majority of the Alloy 82/182 weld material while the weld overlaid joints maintain structural integrity. The remaining structural material at the weld overlaid locations is Alloy 52M which is resistant to PWSCC. Considering the new weld joint consists of both Alloy 52M and Alloy 82/182 materials, it would even more conservative to apply this same penalty factor throughout both

materials. Therefore, a penalty factor of 1.0 for PWSCC is utilized for the thickness of the Alloy 690/52/152 material (consistent with Standard Review Plan (SRP) 3.6.3, Section III.3). The penalty factors of 1.69 and 1.0 are combined by weighted averages utilizing the appropriate penalty factor for the radial thickness dimension of material the flaw is extended through for a surface leak-before-break leakage path. This method results in an effective penalty factor of 1.44.

This method is believed to be appropriate and conservative based on the following considerations. The mechanical material properties of Alloy 82/182 and Alloy 52M are essentially the same. From a stress standpoint there are no interface differences to consider at the transition between the Alloy 82/182 base layer and the Alloy 52M weld overlay layer. The weld with the overlay can be addressed as a thicker layer of material. Absent the additional PWSCC crack morphology affects, the leakage flaw size for the Alloy 52M weld overlay will be appropriately smaller than that for the base weld. The leakage flaw without the penalty factor is a conservative estimation of the leakage flaw size for the weld overlay itself, the only difference being the effect of thickness. The leakage flaw using fatigue crack morphology parameters is determined first and then increased by the penalty factor to obtain the PWSCC leakage flaw size. The assumed flaw size determined a leakage flaw of 2.5 gpm (using a margin of 10 on leak detection). The leak rate for the overlay would be greater than 2.5 gpm since overlay crack morphology is smoother than the original weld but is limited by the leakage inventory of 2.5 gpm from the original weld. These elements are combined primarily because the assumed LBB flaw would have to penetrate the Alloy 82/182 material for a "potential" leakage path. This method represents a conservative approach that demonstrates leakage detection capability based on a highly unlikely leakage path assumption. Also the post SWOL residual stresses demonstrate that the inside surface of the pipe will be in a compressive stress zone. Therefore, the SWOL application will prevent any crack initiation and arrest any PWSCC cracks at the inside surface.

In summary, the use of a 1.69 penalty factor for original Alloy 82/182 material taken from Reference 5-6 (and PVP2005-71200) is judged to be conservative. This is based on the fact that the limited data would tend to skew the results in an overly conservative manner. From the results provided in Reference 5-5, a penalty factor of 1.37 to account for PWSCC is considered to be more realistic for leakage flaw size determination. The Waterford 3 surge line evaluation for WCAP-17187-P results in a penalty factor of 1.44 which is in excess of the 1.37 penalty (Reference 5-5). Therefore, the approach contained in WCAP-17187-P provides conservative results that bound the leakage flaw effects of PWSCC.

Additional application of an alternate methodology to predict the leakage flaw size is not believed to provide appreciable different or more conservative results.

**RAI N-10 (Round 2)** The staff does not understand the argument that limited data suggests overly conservative results as stated in the 5$^{th}$ paragraph of the licensee's response. From a statistics standpoint, limited data can be used to make a good estimate of the mean. However, limited data suggest that the lack of knowledge uncertainty is large, thus producing a large scatter in the predicted distributions. Obtaining more data will decrease this uncertainty and reduce the scatter, but will not have a large impact on the mean.

The experiments that were used to benchmark the KRAKFLO predictions were conducted by Battelle. The engineers that conducted those experiments have repeatedly discussed the testing issues associated with those experiments. For instance, the crack opening displacement (COD) measurements made during the leakage experiments were taken near the crack tip and not at the crack centerline. Therefore, the actual experimental crack opening was much larger than measured in the experiments. If an analysis was used to predict these experiments and assuming the COD (actually measured off center) was measured at the centerline, the analyses would under predict the effects of morphology, i.e., for the same leak rate, and crack length, a larger COD would require more torturous crack morphology parameters than a smaller COD. Therefore, the factor of 1.37 under predicts the effects of crack morphology parameters. Since the actual centerline COD measured in the Battelle experiments is not known, it is impossible to quantify how much the 1.37 under predicts the effects of morphology. Discuss whether your analysis is conservative.

**Response:** Several industry studies have been performed to address the crack morphology affects from Alloy 82/182 materials due to PWSCC. In our previous response to this question, Entergy referenced the use of a penalty factor of 1.69 that was applied to the base susceptible weld layer of Alloy 82/182 for the hot leg and pressurizer surge line nozzles. This penalty factor was obtained from a study performed by Rudland, Wilkowski, et. al (Reference 5-6 of WCAP-17187-P). Based on the weighted averaging of the base layer and the weld overlay of Alloy 52M, an average penalty factor of 1.44 was obtained. This was compared against a study performed by Nana and Yoon (Reference 5-5 of WCAP-17187-P) which determined using the KRAKFLO leak rate program that concluded a mean average penalty factor of 1.37. The comparison to the latter study which concluded a penalty factor of 1.37 was only to represent that the application of a penalty factor of 1.69 for the PWSCC susceptible layer and the average penalty factor of 1.44 provided conservative results. The application of the penalty factor of 1.69 was also considered to be very conservative as discussed in EPRI MRP-140. Further, if a 1.69 penalty factor were to be applied for both the Alloy 82/182 and Alloy 52M weld layers, the leakage flaw size would only be increased by 17% which is within the currently analyzed LBB margins contained in WCAP-17187-P. Therefore, Entergy concludes that the use of a PWSCC penalty factor of 1.69 for increasing the size of the leakage flaw for the base layer is conservative.

**RAI N-11** Page 5-3,

(1) Explain how the leakage crack in the weld overlaid DMW and in the weld overlay is modeled, how the degradation mechanism in the overlay and in the DMW is assumed, and what input was used for the leakage crack model to predict leak rates.

(2) If a computer code is used to calculate the leak crack size, describe the computer code that performed the calculation and discuss the level of validation conducted for this software.

**Response:** (1) As discussed on Page 5-3 of WCAP-17187-P, an effective penalty factor of 1.44 was applied which provides conservative leakage flaw sizing. This approach is believed to provide bounding results and no additional modeling techniques were considered necessary to obtain PWSCC leakage flaw sizing.

(2) A separate computer model is not considered necessary to represent the PWSCC leakage flaw size determination.

**RAI N-12** Page 6-6, Explain why Table 6-3 does not include stability results for Node 10 (the hot leg to surge line nozzle).

**Response:** Table 6-3 provides stability results based on J-integral evaluations. Node 10 has the Alloy 82/182 and Alloy 52M which are high toughness materials. The stability analysis is based on the limit moment method which is appropriate for these materials and J-integral analysis is not necessary at this location.

**RAI N-13** Pages 6-9, 6-10, 6-11, and 6-12, Discuss how the curves on these pages were constructed.

**Response:** Figures 6-3 through 6-6 graphically represent the various limit moment versus the critical flaw sizes using the equations shown in Appendix A and in Section 6.2. They also illustrate the circumferential critical flaw size using the governing faulted loads.

**RAI N-14** Page A-1, Cite reference(s) from which equations (A-1 and A-3) were taken.

**Response:** Appendix A provides the limit moment equations which are also provided in Section 6.2. These are Westinghouse derived equations similar to methodology and the equations provided in WCAP-17187-P, Reference 6-2 and Section XI, Appendix C of the ASME Code.

**RAI N-15** The NRC staff plans to use the PICEP computer code from the report, "Pipe Crack Evaluation Program," Electric Power Research Institute, EPRI NP-3596-SR, Revision 1, to perform a confirmatory analysis. The NRC staff requests the following information at Nodes 10, 20, 70, and 75 that were analyzed in WCAP-17187-P:
(a) primary membrane stress and bending stress,
(b) normal operating pressure,
(c) 0.2% offset yield stress,
(d) yield strain,
(e) Ramberg-Osgood exponents (n) and coefficient (alpha),
(f) Is the fluid saturated or sub-cooled before exiting the crack,
(g) fluid stagnation pressure and temperature,
(h) height of protrusion of the roughness grain from surface (in inches).

**Response:** The following parameters were used in the Waterford 3 analysis performed in WCAP-17187-P:

a) Primary stress, bending stress: See attached Table 1 for R-7 response.

b) Normal operating pressure = 2250 psi

c) 0.2% offset yield stress for cast austenitic stainless steel (CASS) and stainless steel (SS) weld materials are given in WCAP-17187-P, Table 4-1 and the Alloy 82/182 and 52M are given in Table 4-2.

d) Yield strain = yield stress/ E where yield and E are given in WCAP-17187-P, Tables 4-1 & 4-2.

e) Ramberg-Osgood law parameters

- CASS material $\alpha = 1.0202$, $n = 5$
- SS weld material $\alpha = 3.938$, $n = 5$
- Alloy 82/182 material $\alpha = 1.145$, $n = 9.759$

Note: for the PICEP leak rate calculations, $\alpha = 0$ should be used since the normal stresses are in the elastic range.

f) Fluid status: sub-cooled.

g) Fluid stagnation P = 2250 psi, T= 653° F (for the leak rate calculation the limiting normal operating case parameters)

h) Height of protrusion of roughness of grain = [see WCAP-17187-P, section 5.3]. Note: PICEP uses 200 micro-inches surface toughness.

**RAI R-1** Section 2.2, last two lines on page 2.2. It is mentioned that the temperature and pressure are maintained within a narrow range. Provide quantitative values of the ranges.

**Response:** Based on Waterford 3 operating procedures, the pressurizer pressure controller is set to maintain a setpoint value of 2250 PSIA (steady state operation). The procedurally allowed range for controlling RCS pressure is 2175 psia to 2265 psia. The Tech Spec range is 2125 psia to 2275 psia.

As a result of controlling $T_{cold}$ and pressurizer pressure within the procedural requirements, a surge line temperature range of 641.5°F ±1.5°F is observed under steady state conditions.

**RAI R-2** Section 2.3, Provide any prior occurrences of fatigue cracking or primary water stress corrosion cracking in this piping system.

**Response:** See response for N-2

**RAI R-2 (Round 2)** The response to RAI R-2 refers to the response to RAI N-2. However, the response to RAI N-2 does not address occurrences of primary water stress corrosion cracking (PWSCC) in the pressurizer surge line. Therefore, the response to RAI R-2 needs to be revised to address prior occurrences of PWSCC in the pressurizer surge line.

**Response:** No PWSCC flaws have been identified in the Waterford 3 surge line nozzles. The weld overlays were applied to the surge line hot leg and pressurizer nozzle joints only as a preemptive mitigation for the potential of PWSCC flaw leakage. The weld overlays and base Alloy 82/182 layer were examined by ultrasonic testing (UT) as part of the placement of the weld overlays in May 2008. The UT examinations did not reveal any PWSCC cracking or indications. These examinations were reported in Entergy letter dated May 29, 2008 (ADAMS Accession No. ML081540252).

**RAI R-3** Section 2.2, Provide quantitative information about historic frequencies on water hammers in surge piping.

**Response:** Reactor coolant system is designed and operated to preclude any voiding condition in normally filled lines. There should not be any waterhammer in the surge line piping system. This was confirmed based on a review of the Waterford 3 condition reporting system which did not reveal any historical occurrences of water hammer.

**RAI R-4** Page 3-1, Loads for Fracture mechanics analysis. In conducting the piping stress analyses for determination of loads, was the effect of the weld overlay included in the analyses? This effect may be minimal for normal operating loads, but may have a larger effect on the safe shutdown earthquake (SSE) load calculation.

**Response:** The effects of the weld overlays on the Waterford 3 surge line were performed by Structural Integrity Associates (SIA) as part of the surge line pipe nozzle weld overlay installation. The results of the analysis for surge line pipe mass and shrinkage due to surge line weld overlays are provided below:

| Loads | Pzr Nozzle | Hot Leg Nozzle |
|---|---|---|
| Change in mass (relative to the mass of the pipe, nozzle, and water) | 1.1% | 2.1% |
| Surge line pipe axial shrinkage (due to weld overlay shrinkage) | 0.0175" ave. | 0.042" ave. |

Additional loads that would be imparted by the increased surge line pipe were not considered to significantly affect the existing pipe stress analyses including loads from dynamic excitation due to the SSE. The configuration of the vertically orientated axial pipe shrinkage on the "floating" [non-restrictive movement] design of the surge line pipe from the pressurizer to the hot leg surge nozzle was bounded by the measurement tolerances for the surge line restraint gaps. These affects were concluded to be acceptable given the length of the surge line piping between the pressurizer and hot leg surge nozzle and the elbows in the surge line pipe routing geometry.

**RAI R-4 (Round 2)** The staff believes that the weld overlay (WOL) significantly stiffens the Alloy 82/182 dissimilar metal (DM) weld joint. This stiffness should affect the stresses calculated at that location. Discuss whether the stiffness has been evaluated in the updated leak-before-break analysis of the pressurizer surge line. If yes, discuss the results. If no, justify why stiffness of the WOL was not evaluated.

**Response:** The Waterford surge line Alloy 82/182 welds have the pre-emptive weld overlay at the nozzle to safe-end joint. The surge line pipe stress calculation models the pipe stresses from safe-end to pipe joint for both anchored ends of the surge line. The nozzle pipe to safe-ends were conservatively selected as anchor points to maximize piping loads. The additional stiffness of the nozzle to safe-end from the weld overlay presents no change to pipe stresses due to the selection of the nozzle safe-end to pipe as the anchor point.

**RAI R-5** Specify the computer software that was used to conduct the piping stress analysis. Describe how the weld overlay was modeled in the piping stress analysis.

**Response:** The analysis performed for the Waterford-3 (W3) surge line (and supports) used the PIPESTRESS computer code. PIPESTRESS is a verified piping code used in the nuclear industry for ASME Code analysis of piping systems. PIPESTRESS was used for all of the Waterford 3 RCS attached piping analyses performed for extended power uprate (EPU) and EPU with replacement steam generator conditions.

Weld overlays on the nozzles were not included in the piping analyses. The weld overlay is evaluated as part of the nozzle stress analysis using end loads from the piping analyses. Similar to the results performed by SIA, Westinghouse experience with weld overlays has determined that the two effects of nozzle weld overlays on the attached piping are added nozzle weight due to the weld material deposits, and axial shrinkage of the nozzles. These effects are negligible when considering piping systems such as the surge line. The added weight at what are essentially anchor points for the subsystem has minimal effect on the response of piping of this size. Furthermore, surge lines are designed for maximum flexibility (e.g., they are relatively long and have many bends) in order to accommodate the thermal contraction and expansion of the line that occurs during the course of normal operation. This added flexibility further mitigates any weld overlay induced affects on the surge line.

**RAI R-5 (Round 2)** The WOL significantly stiffens the DM weld joint. For elastic piping analyses, it increases the section modulus, which should change the calculated loads for the displacement controlled conditions. Because the weld overlay was not included in the piping analysis, justify the piping loads used in the fracture mechanics analysis (critical crack size and leakage crack size) are conservative.

**Response**: As noted in the response to RAI R-4 (Round 2) above, the selection of the anchor points for the surge line LBB pipe stress analysis conservatively maximizes the displacement calculated loads. These maximized loads effectively force a reduced critical crack size with lower crack leakage. The maximized loads from the safe-end to pipe anchor point were applied to the Alloy 82/182 weld at the safe-end to nozzle joint. Therefore, the loads are conservative as modeled.

**RAI R-6** Axial shrinkage of the weld overlay can cause a tensile axial stress in the rest of the piping system when the weld overlay is in-situ with the piping system connected to the pressurizer and hot leg. How is the axial shrinkage accounted for in the pipe stress analyses?

**Response:** The effects of the surge line pipe nozzle axial shrinkage were evaluated and determined to not adversely impact the existing surge line pipe stress analyses. See

response to RAI R-4 and R-5 above. These as-built measurements confirm the minor contribution from the axial shrinkage that occurs over the thirty-eight foot distance between the hot leg surge line nozzle and the pressurizer surge line nozzle.

**RAI R-7** (1) Clarify the procedure for choosing the critical location for conducting the LBB analyses. In Section 3.1, it is stated that the pipe locations were selected based on the magnitude of the moments and their proximity to elbows. Node 70 was chosen as the worst case. However, for Load Case A in Table 3-5, Node 20 had higher moments than that of Node 70.

(2) To aid in necessary confirmatory calculations, provide all load components (i.e., moments in the x, y, and z directions and Fx) for each ASME loading category case (A, B, C and D) for Nodes 70, 75, 80, 10, 20, 25, 45 and 55.

**Response:** (1) The most critical LBB analyses location was chosen based on the highest faulted stress from all the weld locations. As shown in Table 3-5, Node 70 has the highest faulted stress (Case F) and therefore is the most limiting location for the LBB analyses. Stability analyses results (Table 6-3 and Table 8-1) show that Node 70 is the most limiting locations. For Load Case A in Table 3-5, Node 20 had higher moment than that of Node 70. Higher normal moments and stresses at Node 20 provide lower leakage flaw and higher flaw size margin. The individual loading cases at each location are considered separately for the LBB leakage and stability analyses. The approach taken in Section 3.1 was supported from the pipe stress analysis.

(2) As requested, combined moments for the x, y, and z directions and Fx for each LBB loading category case of cases A, B, C and D for Nodes 70, 75, 80, 10, 20, 25, 45 and 55 are provided in Table 1 below.

**RAI R-7(2) (Round 2)** Table 1 provides various loads for various nodal points. However, loads for Node 10 in Table 1 do not include the thermal loads. Please include all load components (deadweight, thermal expansion, etc). Please forward these loads to the staff as soon as possible (informally to expedite the process) so that the staff can perform its confirmatory analysis expeditiously.

**Response**: Table 1 below has been supplemented for Case D of Node 10 (hot leg surge line nozzle) to include a thermal loading component (Case D for Node 10 as previously provided in Table 1 contains the deadweight loads). The revised stresses are also provided for Node 10, Case D based on the additional thermal loadings. Node 10 Cases A, B, and C are unchanged from the previous information provided since they included their specified loads.

**RAI R-8** Page 3-10. Justify the acceptability of calculating the critical flaw size in Alloy 182 welds without any displacement-controlled loads such as thermal expansion. In Materials Reliability Program, MRP-216, report, published by the Electric Power Research Institute, analyses were conducted by both Structural Integrity Associates and Quest Reliability that suggested that some of the displacement controlled loads can be eliminated from the calculation of through-wall crack stability. In fact, the work by Quest suggests that for relatively long flaws, only about 50% of the applied moment would be relieved. In the MRP-216 work, since there was still question about how much of the displacement-controlled loads were used in critical crack calculations, the thermal expansion loads were assumed to contribute to the through-wall crack stability.

**Response:** The critical flaw size in Alloy 182 welds is calculated using plastic instability as a failure mode, also known as ductile limit load. This approach has been demonstrated to be accurate in predicting failures of high toughness materials in hundreds of pipe tests conducted world-wide.

The theory of plastic instability states that the component will fail in the presence of a crack when the remaining ligament becomes entirely plastic. When this happens, all displacement-controlled stresses, such as thermal and residual stresses relax, and therefore do not affect the failure. This occurs in all the structural materials used in the primary coolant system of a PWR, and is invariant of temperature in stainless steels and Nickel-based alloys such as Alloy 182 welds. This is the methodology used in Appendix C of ASME Section XI, and documented in the technical basis documents which support it.

In MRP-216, section 5.3, the first paragraph states the following:

> *The results of this study support the conclusion that the surge nozzle piping thermal loads are completely relieved prior to nozzle rupture, since the supportable crack plane rotation is greater than the imposed rotation due to thermal expansion.*

In MRP-216, the normal piping thermal loads were used to add conservatism to expeditiously resolve an issue for the industry. As stated in the quote above, there was no technical need to include the thermal loads.

This conclusion is consistent with the wording in the standard review plan, SRP 3.6.3 (Rev. 1, March 2007). Here, for base metal and TIG welds, which have high toughness similar to Alloy 82/182, no thermal stress is used in the calculation of the critical flaw size, as shown in equation (7) on page 3.6.3-11.

**RAI R-8 (Round 2)** The staff does not agree with the argument of the relaxation of the displacement stresses as discussed in the second paragraph of the response. For through-wall cracks, most of the displacement controlled loads are relaxed, and the driving force does decrease. However, the work by Ted Anderson in MRP-216 suggests the displacement controlled moments are not fully relaxed until the crack length is significantly long, i.e., 70-80% of circumference. These results suggest that there is uncertainty to whether the displacement controlled loadings are fully relaxed and whether this assumption is conservative. The licensee needs to provide additional technical basis to support the argument that the displacement controlled loads are not needed in the critical crack size calculation.

**Response**: Various industry studies have been conducted regarding the affects of displacement controlled loads on crack opening displacement. Even though some uncertainty exists

as to when the majority of the displacement controlled loads relax, it is generally understood that these loads are relaxed quickly, well before nozzle failure. Additional review of EPRI MRP-216 reveals that a crack length of 58% of the circumference can also become fully relaxed under the displacement controlled moments. For other smaller lines, the crack length can be as low as 36%. This is presented in Appendix B of MRP-216.

Based on SRP 3.6.3, Z-factors are not required for high toughness materials when determining critical flaw sizing. As discussed in MRP-140, Alloy 82/182 is classified as a high toughness material comparable to base metals and TIG welds. Therefore, the secondary stresses need not be considered in the limit load analysis. This approach is further supported by ASME Section XI and Section III where thermal expansion stresses are not considered for high toughness materials (i.e. GTAW weld process). However, for the Waterford surge line analysis, a Z-factor was conservatively applied which addresses uncertainties from secondary thermal loads. Therefore, we believe that the approach applied for the Waterford 3 critical flaw sizing determination provides adequate conservatism.

**RAI R-9** Page 4-1, Tensile material properties. Clarify why ambient, not operating, temperature material properties (with temperature correction), taken from the Battelle database, were used in the analyses. In many cases, operating temperature material properties are also available in the database.

**Response:** Yield and ultimate strength data from certified material test report (CMTR) information is available only at room temperature. Hence NRC Battelle stress-strain curve at room temperature was considered for R-O law fit. Temperature variation for yield strength, ultimate strength and modulus of elasticity shown in Tables 4-1 and 4-2 were considered.

**RAI R-9 (Round 2)** The response does not answer the question. The staff suggests that the Battelle data (both at room temperature and operating temperature) that corresponds to the Certified Material Test Report (CMTR) for this material be used.

**Response**: The NRC Battelle report on PIFRAC material database, "Pipe Fracture Encyclopedia" (Volume 1, 1997) has stress-strain properties for CASS base materials at temperatures of 20°C (68°F), 149°C (300°F), and 288°C (550.4°F). A plot of the true stress-strain data for PIFRAC samples A37-1 through A37-6 is shown in Figure 1 below. This data includes two samples at each of the three temperatures. The strain range of interest for the LBB applications is from 0% to 5%. This material data is approximated using the Ramberg-Osgood (R-O) law equation:

$\xi = \sigma/E + \alpha(\sigma_0/E)(\sigma/\sigma_0)^n$ , where

$\xi$ = strain
$\sigma$ = stress
E = Young's modulus of elasticity
$\alpha$ and $n$ are material constants

This form of the material curve idealization has limited parameters to represent the actual material stress-strain curves. In the low strain range of interest, the data in Figure 1 shows similar trends with temperature. The room temperature curve was applied to fit the R-O law, then used for all temperatures of interest keeping the

parameters α and n constant but represented the temperature variation through the reference stress ($\sigma_0$) (yield strength of the material) and the modulus of elasticity (E). This variation is taken from the ASME Code. The yield strength of the actual material in the Waterford Unit 3 surge line at room temperature is obtained from the actual CMTRs. Yield strength at higher temperatures is obtained by scaling CMTR values proportionately with the ratio of the ASME Code yield strength at ambient temperature to the evaluation temperature.

The yield stress inferred from the PIFRAC data was compared to the yield stress for the actual surge line materials. It was observed that the room temperature yield strength of the CASS material in PIFRAC is significantly lower than the CMTR values of the actual material. Also, the yield stress from the limited amount of PIFRAC data variation with temperature is inconsistent and has no trend, as the data at two higher temperatures, 149°C and 288°C, are almost identical and do not show any temperature variations. The trend of yield stress of the PIFRAC samples with temperature was not smoothly decreasing as expected. For these reasons, the PIFRAC data cannot be used directly. However, the shape of stress versus strain as represented by the R-O law fit curve can be scaled to the CMTR yield stress at room temperature. Then, the curves at higher temperatures are obtained by scaling the room temperature curve by the ratio of the ASME Code yield stress at the evaluation temperature over the yield strength at room temperatures.

This alternate approach is consistent with higher temperatures given the similarity of the PIFRAC stress-strain properties in the low strain range. This approach has also been verified by using the R-O law fit to the actual PIFRAC stress-strain curve data at higher temperatures of 149°C (300°F), and 288°C (550°F) and was observed to represent this data appropriately thereby supporting the methodology used.

A similar approach to the CASS material was also used for the stainless steel (SS) weld materials. The ambient temperature stress-strain properties available for sample A8-1-1 and A8-1-2 at temperature of 22°C (71.6°F) were fitted to R-O law, and then extrapolated to higher temperatures using the ASME Code scale factors. The resulting R-O law was also checked for the PIFRAC data available for sample A8-1-4 at 288°C (550.4°F) and found to be appropriately represented.

**RAI R-10** Page 4-4, Describe how the tearing modulus is calculated. For the J-R power-law representation, what crack extension was used to calculate the toughness slope dJ/da?

**Response:** The J-curve is represented by:

$$J_R = \beta(\Delta a)^m$$

Table 4-4 lists β and *m* for CASS material.

Tearing modulus is computed from

$$T = E/\sigma_f^2 \, (dJ/da)$$

Material modulus of elasticity (E) and flow stress ($\sigma_f$) computed from Table 4-1 were used in computing the tearing modulus (T). Crack extension is assumed as 0.39 in (10mm) at $J_{max}$.

**RAI R-11** Page 4-6, Table 4-1, shows material properties (yield and ultimate strength and modulus of elasticity), for Node 20 taken at 333ºF. Page 4-9, Table 4-5, shows fracture toughness values for Node 20 taken at 333 degrees F. Justify why materials properties and fracture toughness values for Node 20 are presented for 333 degrees F because under operating conditions D & E, the temperature at Node 20 should be above 333 degrees F.

**Response:** Refer to response for RAI R-15.

**RAI R-12** Page 5-3, second to the last paragraph. Justify the conclusion that the leakage size flaws are conservative. The licensee states that the weld residual stresses (WRS) from the weld overlay (WOL) will cause compressive stresses on the inside diameter surface, thus making the calculation conservative. From a flaw tolerance standpoint, the WRS will cause the crack faces to close, thus reducing the crack opening and creating a longer leakage flaw size. Therefore ignoring the WRS would be non-conservative.

**Response:** The approach taken regarding residual stresses was for a defense in depth perspective to emphasize that surface cracking will not initiate due to the compressive stresses on the inside diameter of the pipe.

For the LBB analysis, hypothetical through-wall flaws are postulated in order to calculate the leakage flaw size and critical flaw size. The residual stresses are localized in nature and are self-relieving for the postulated through-wall flaws used in the LBB analyses. SRP 3.6.3 does not require residual stresses to be included in the analysis.

**RAI R-12 (Round 2)** When NRC Standard Review Plan (SRP) Section 3.6.3 was written, the effects of weld residual stresses (WRS) on the leakage were unknown. The staff disagrees that the WRS are relieved by the presence of the through wall crack. The staff has performed analyses that demonstrate that the WRS changes the crack opening displacement, which will affect leak rate. Ignoring WRS may be consistent with SRP Section 3.6.3 but it is not conservative. The licensee needs to provide additional technical basis show why WRS do not need to be used in the fracture mechanics analysis.

**Response**: Based on NUREG/CR-6300, "Refinement and Evaluation of Crack-Opening-Area Analyses for Circumferential Through-Wall Cracks in Pipes" (April 1995), there will be insignificant impact on the leakage flaw size due to weld residual stresses. Using Table 8.3 of NUREG/CR-6300, the impact of residual stresses on the COD is roughly 3.3 to 4.4% which is within engineering calculation accuracy. Therefore, weld residual stresses does not represent a significant load in the LBB analysis. These stresses have also not been considered at other non-Alloy 82/182 weld locations.

Other more recent studies have been conducted that considered the impact of weld residual stresses on COD such as documented in NUREG/CR-6765, "Development of Technical Basis for Leak-Before-Break Evaluation Procedures" (May 2001) and NUREG/CR-6837, "The Battelle Integrity of- Nuclear Piping (BINP) Program Final Report" (June 2005). NUREG/CR-6837 indicates that the effect of residual stresses

on COD is especially pronounced for thin-wall pipe operating at low stress level. Even though the affect on COD due to weld residual stresses may vary, the general conclusions reached is that for most practical applications, the effect of weld residual stresses on the COD, by itself, was not a major contributing factor for LBB analyses (i.e., less than a 15 to 20 percent effect on the margin or crack size). The subsequent revision (Revision 1) to SRP 3.6.3 did not require the affect of weld residual stresses be included in LBB leakage flaw determination methods.

**RAI R-13** Page 6-3, Limit Moment Method. Confirm that the applied moments were multiplied by the applicable Z-factor for determining critical flaw size.

**Response:** Yes, it is confirmed that the applied moments were multiplied by the applicable Z-factor for determining the critical flaw size.

**RAI R-14** Page 6-3, For the overlaid Alloy 82 weld, which diameter was used in the Z-factor calculation (e.g., the outside diameter before or after the overlay)?

**Response:** For the overlaid Alloy 82 weld, the outside diameter after the overlay was applied was used in the Z-factor. Please note that the Z-factor for the Alloy 52M material is 1.0 however, conservatively the same Z factor for Alloy 82/182 weld was also applied for the Alloy 52M material and the diameter was used as the outside diameter after the overlay. Therefore, the calculated critical flaw size with the Z-factor is conservative.

**RAI R-15** Page 6-5, Demonstrate that for Nodes 70, 75 and 20, faulted load case F is the limiting case. For Node 20, at 333 degrees F, this case may not be limiting, since the temperatures will be higher for other load cases and the strengths will be lower, and the critical flaw sizes may be shorter.

**Response:** As shown in Table 3-5 (page 3-9) of the WCAP report, the total stresses for the loading case F are the highest of the applicable loading cases; therefore Case F is the limiting case.

For Node 20 Case F at 333° F is the limiting case. At Node 20, the faulted total stresses (Table 3-5) are:

Case F = 25.99 ksi

Case D = 13.34 ksi

Case E = 13.98 ksi

The stress ratio between Case F/Case D is 1.95 and the stress ratio between Case F/Case E is 1.86.

Base material properties comparison

For Node 20, base material properties are:

$\sigma_y$ = 37.52 ksi (333°F)

$\sigma_y$ = 29.41 ksi (653°F)

$\sigma_y$ ratio = 37.52/ 29.41= 1.28.

$\sigma_u$ = 83.77 ksi (333°F)

$\sigma_u$ = 82.46 ksi (653° F)

$\sigma_u$ ratio = 83.77/ 82.46= 1.02

Modulus of Elasticity (E) = 26970 ksi (333 °F)

Modulus of Elasticity (E) = 25080 ksi (653 °F)

E ratio is = 26970/ 25080= 1.08

Weld material properties comparison

For Node 20, weld material properties are:

$\sigma_y$ = 42.89 ksi (333° F)

$\sigma_y$ = 33.63 ksi (653° F)

$\sigma_y$ ratio = 42.89/ 33.63 = 1.28.

$\sigma_u$ = 81.40 ksi (333° F)

$\sigma_u$ = 76.51 ksi (653° F)

$\sigma_u$ ratio = 81.4/ 76.51 = 1.06

Modulus of Elasticity (E) = 26810 ksi (333 ° F)

Modulus of Elasticity (E) = 25030 ksi (653 ° F)

E ratio is = 26810/ 25030= 1.07

Conclusion

The material properties change ratio of 1.28 (maximum factor) is a lot lower than the stress change ratio of 1.86 (minimum factor). Therefore, stability calculations using Case F using 333 ° F governs for Node 20 over Case D or E. Similarly for Node 70 and Node 75 faulted load Case F also governs.

**Table 1 Combined Moments for Each Loading Category in Response to RAI R-7**

| NODE 10 | Loadings | | | | |
|---|---|---|---|---|---|
| | Fx (kips) | Mx (in-kips) | My (in-kips) | Mz (in-kips) | M-SRSS (in-kips) |
| CASE A | 176.607 | -745.656 | -151.428 | -35.736 | 761.715 |
| CASE B | 176.585 | -757.056 | -385.080 | -3.432 | 849.372 |
| CASE C | 181.103 | -908.328 | -2103.072 | 540.876 | 2353.831 |
| CASE D | 183.046 | 209.664 | 178.740 | 160.824 | 319.016 |
| CASE D Note 1 | 184.285 | 960.012 | 405.324 | 171.852 | 1056.15 |

| NODE 10 | Stresses (ksi) | | |
|---|---|---|---|
| | Membrane | Bending | Total |
| CASE A | 2.04 | 3.25 | 5.29 |
| CASE B | 2.04 | 3.63 | 5.66 |
| CASE C | 2.09 | 10.05 | 12.14 |
| CASE D | 2.11 | 1.36 | 3.47 |
| CASE D Note 1 | 2.13 | 4.51 | 6.64 |

| NODE 20 | Loadings | | | | |
|---|---|---|---|---|---|
| | Fx (kips) | Mx (in-kips) | My(in-kips) | Mz(in-kips) | M-SRSS |
| CASE A | 187.241 | -745.656 | 57.804 | 55.812 | 749.973 |
| CASE B | 187.219 | -757.056 | 25.524 | -175.632 | 777.581 |
| CASE C | 191.737 | -908.328 | -601.884 | -1989.156 | 2268.053 |
| CASE D | 194.409 | 960.012 | 163.140 | 180.108 | 990.291 |

| NODE 20 | Stresses (ksi) | | |
|---|---|---|---|
| | Membrane | Bending | Total |
| CASE A | 4.40 | 6.64 | 11.04 |
| CASE B | 4.40 | 6.88 | 11.29 |
| CASE C | 4.51 | 20.08 | 24.59 |
| CASE D | 4.57 | 8.77 | 13.34 |

| NODE 25 | Loadings | | | | |
|---|---|---|---|---|---|
| | Fx (kips) | Mx (in-kips) | My (in-kips) | Mz (in-kips) | M-SRSS |
| CASE A | 203.814 | -83.628 | -771.492 | -248.040 | 814.689 |
| CASE B | 203.958 | -51.384 | -782.904 | -18.780 | 784.813 |
| CASE C | 197.743 | 673.308 | -836.904 | 1825.284 | 2117.880 |
| CASE D | 205.744 | 177.300 | 930.540 | 309.348 | 996.512 |

| NODE 25 | Stresses (ksi) | | |
|---|---|---|---|
| | Membrane | Bending | Total |
| CASE A | 4.79 | 7.21 | 12.01 |
| CASE B | 4.80 | 6.95 | 11.75 |
| CASE C | 4.65 | 18.75 | 23.40 |
| CASE D | 4.84 | 8.82 | 13.66 |

| NODE 45 | Loadings | | | | |
|---|---|---|---|---|---|
| | Fx (kips) | Mx (in-kips) | My (in-kips) | Mz (in-kips) | M-SRSS |
| CASE A | 203.814 | 153.936 | -54.144 | -1380.156 | 1389.769 |
| CASE B | 203.958 | 194.748 | 178.464 | -1393.140 | 1417.962 |
| CASE C | 201.867 | 456.012 | 1870.008 | -1141.344 | 2237.754 |
| CASE D | 205.262 | 182.568 | 133.068 | 1471.704 | 1488.943 |

| NODE 45 | Stresses (ksi) | | |
|---|---|---|---|
| | Membrane | Bending | Total |
| CASE A | 4.79 | 12.30 | 17.10 |
| CASE B | 4.80 | 12.55 | 17.35 |
| CASE C | 4.75 | 19.81 | 24.56 |
| CASE D | 4.83 | 13.18 | 18.01 |

| NODE 55 | Loadings | | | | |
|---|---|---|---|---|---|
| | Fx (kips) | Mx (in-kips) | My (in-kips) | Mz (in-kips) | M-SRSS |
| CASE A | 192.437 | 99.240 | -120.852 | -1022.244 | 1034.136 |
| CASE B | 192.472 | 350.460 | -92.784 | -1033.128 | 1094.890 |
| CASE C | 196.085 | 2273.544 | 232.008 | -1241.556 | 2600.825 |
| CASE D | 193.316 | 149.796 | 140.976 | 1104.900 | 1123.885 |

| NODE 55 | Stresses (ksi) | | |
|---|---|---|---|
| | Membrane | Bending | Total |
| CASE A | 4.53 | 9.16 | 13.68 |
| CASE B | 4.53 | 9.69 | 14.22 |
| CASE C | 4.61 | 23.03 | 27.64 |
| CASE D | 4.55 | 9.95 | 14.50 |

| NODE 70 | Loadings | | | | |
|---|---|---|---|---|---|
| | Fx (kips) | Mx (in-kips) | My (in-kips) | Mz (in-kips) | M-SRSS |
| CASE A | 176.856 | 8.424 | -692.244 | 240.300 | 732.814 |
| CASE B | 176.712 | -7.104 | -696.816 | 531.696 | 876.529 |
| CASE C | 169.632 | 115.260 | -509.184 | 2680.764 | 2731.126 |
| CASE D | 206.202 | 63.132 | 790.680 | 448.572 | 911.250 |

| NODE 70 | Stresses (ksi) | | |
|---|---|---|---|
| | Membrane | Bending | Total |
| CASE A | 4.16 | 6.49 | 10.65 |
| CASE B | 4.16 | 7.76 | 11.92 |
| CASE C | 3.99 | 24.18 | 28.17 |
| CASE D | 4.85 | 8.07 | 12.92 |

| NODE 75 | Loadings | | | | |
|---|---|---|---|---|---|
| | Fx (kips) | Mx (in-kips) | My (in-kips) | Mz (in-kips) | M-SRSS |
| CASE A | 189.227 | 718.068 | 34.248 | 16.968 | 719.084 |
| CASE B | 189.431 | 722.676 | 18.756 | -275.508 | 773.639 |
| CASE C | 190.673 | 519.156 | -98.472 | -2375.832 | 2433.885 |
| CASE D | 194.819 | 845.688 | 92.352 | 271.728 | 893.058 |

| NODE 75 | Stresses (ksi) | | |
|---|---|---|---|
| | Membrane | Bending | Total |
| CASE A | 4.45 | 6.37 | 10.82 |
| CASE B | 4.46 | 6.85 | 11.30 |
| CASE C | 4.48 | 21.55 | 26.03 |
| CASE D | 4.58 | 7.91 | 12.49 |

| NODE 80 | Loadings | | | | |
|---|---|---|---|---|---|
| | Fx (kips) | Mx (in-kips) | My (in-kips) | Mz (in-kips) | M-SRSS |
| CASE A | 178.083 | 718.068 | -645.420 | 101.172 | 970.785 |
| CASE B | 178.287 | 722.676 | -359.640 | 85.740 | 811.759 |
| CASE C | 179.529 | 519.156 | 1838.160 | -59.448 | 1910.992 |
| CASE D | 183.911 | 126.756 | 255.336 | 118.560 | 308.739 |

| NODE 80 | Stresses (ksi) | | |
|---|---|---|---|
| | Membrane | Bending | Total |
| CASE A | 2.05 | 4.15 | 6.20 |
| CASE B | 2.06 | 3.47 | 5.52 |
| CASE C | 2.07 | 8.16 | 10.23 |
| CASE D | 2.12 | 1.32 | 3.44 |

Note 1: This Case D for Node 10 includes additional thermal loadings and stresses

**Figure 1: CASS Stress-Strain Curves from PIFRAC Database**

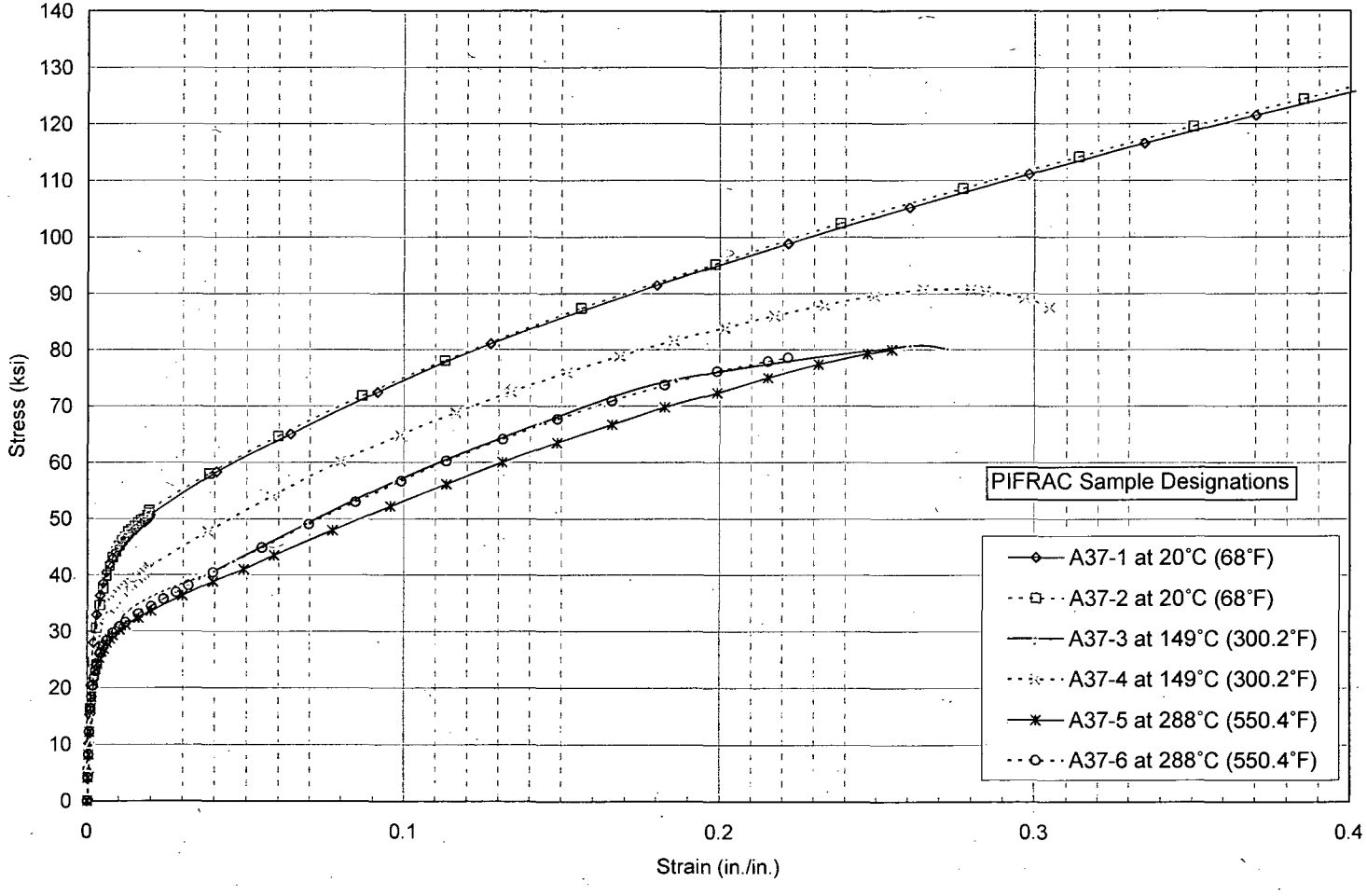

**Figure 2: Stainless Steel Weld S-e Curve from PIFRAC Database**